General and Comparative Endocrinology 281 (2019) 41–48

Contents lists available at ScienceDirect

General and Comparative Endocrinology

journal homepage: www.elsevier.com/locate/ygcen

A Crown-of-Thorns Seastar recombinant relaxin-like gonad-stimulating peptide triggers oocyte maturation and ovulation

Meaghan K. Smith[a], Hoang Dinh Chieu[a], Joseph Aizen[b,a], Benjamin Mos[c], Cherie A. Motti[d], Abigail Elizur[a], Scott F. Cummins[a,*]

[a] GeneCology Research Centre, University of the Sunshine Coast, 90 Sippy Downs Drive, Sippy Downs, Queensland 4556, Australia
[b] The School of Marine Science, Ruppin Academic Centre, 4029700 Michmoret, Israel
[c] National Marine Science Centre, Southern Cross University, 2 Bay Drive, Coffs Harbour, NSW 2450, Australia
[d] Australian Institute of Marine Science (AIMS), Cape Ferguson, Townsville, Queensland 4810, Australia

ARTICLE INFO

Keywords:
Crown-of-Thorns Seastar
Oocyte maturation
Recombinant RGP
Echinoderm

ABSTRACT

The *Acanthaster planci* species-complex [Crown-of-Thorns Seastar (COTS)] are highly fecund echinoderms that exhibit population outbreaks on coral reef ecosystems worldwide, including the Australian Great Barrier Reef. A better understanding of the COTS molecular biology is critical towards efforts in controlling outbreaks and assisting reef recovery. In seastars, the heterodimeric relaxin-like gonad stimulating peptide (RGP) is responsible for triggering a neuroendocrine cascade that regulates resumption of oocyte meiosis prior to spawning. Our comparative RNA-seq analysis indicates a general increase in RGP gene expression in the female radial nerve cord during the reproductive season. Also, the sensory tentacles demonstrate a significantly higher expression level than radial nerve cord. A recombinant COTS RGP, generated in a yeast expression system, is highly effective in inducing oocyte germinal vesicle breakdown (GVBD), followed by ovulation from ovarian fragments. The findings of this study provide a foundation for more in-depth molecular analysis of the reproductive neuroendocrine physiology of the COTS and the RGP.

1. Introduction

The Crown-of-Thorns Seastar (COTS), *Acanthaster planci* species-complex, is an echinoderm of enormous interest due to its impact on coral reef ecosystems around the world. COTS are a major cause of coral reef decline due to their requirement for coral as a source of food and with weaponry consisting of sharp toxic spines, they render themselves unpalatable to most animals (Dana et al., 1972; Kenyon, 2014; Coles et al., 2015). Approaches to limit population numbers are limited since we still have gaps in our understanding of their biology, including reproductive physiology (Johnson et al., 1990; De'ath et al., 2012; Hunt, 2013; Morello et al., 2014; GBRMPA, 2017). However, as an invertebrate deuterostome, the molecular components regulating physiological processes partly resemble that of both invertebrates and vertebrates (Tian et al., 2016; Semmens and Elphick, 2017). For example, echinoderm-like neuropeptides can be found regulating reproductive physiology in invertebrates and vertebrates (Semmens et al., 2016; Tian et al., 2016; Semmens and Elphick, 2017).

Neuropeptides are a class of signalling molecules derived from a larger precursor protein that are primarily produced and secreted from neural tissue (Taghert and Nitabach, 2012). One neuropeptide regarded as a key reproduction regulator in seastars is the relaxin-like gonad stimulating peptide (RGP). RGP was first reported over half a century ago and is responsible for final oocyte maturation (Chaet, 1959). It is heterodimeric, comprised of a two-chain structure including A-chain and B-chain, with disulphide cross-linkages. RGP is presumed to bind to gonad follicle cell G-protein coupled receptors (GPCRs) that stimulate internal Gαs and adenylate cyclase activity (Hirai and Kanatani, 1971; Mita and Nagahama, 1991; Mita et al., 2011a,b; Mita, 2013a,b). The end result is the release of the secondary messenger 1-Methyladenine (1-MeAde), which resumes meiosis of oocytes arrested in prophase (Hirai and Kanatani, 1971; Mita et al., 2011a,b). RGP is only effective upon gonads with oocytes at the final maturation stage (oocyte diameter > 150 μm) (Takahashi and Kanatani, 1981) since the immature gonads lack an active Gαs (Mita, 2013a,b).

In the *Asterias rubens*, *in situ* hybridization experiments have shown that *RGP* localises to solitary cells of the radial nerve cord (RNC) and sensory tentacles (Lin et al., 2017). Our previous investigation into neuropeptides present in the COTS has demonstrated that *RGP* is most abundant in the sensory tentacle (Smith et al., 2017), although this was

* Corresponding author.
E-mail address: scummins@usc.edu.au (S.F. Cummins).

https://doi.org/10.1016/j.ygcen.2019.05.009
Received 2 October 2018; Received in revised form 4 May 2019; Accepted 14 May 2019
Available online 15 May 2019

observed on a single individual. The RGP is processed from a precursor protein, involving prohormone convertase processing at dibasic cleavage sites then complex folding due to the heterodimerisation of cysteine-rich chains. As such, the RGP may be difficult to accurately chemically synthesized or produced through heterologous expression systems [e.g. relaxin/insulin-like synthetics (Thalluri et al., 2018)]. An *Asterina (=Patiria) pectinifera* RGP has been synthesised, including disulphide bonded chains-A and -B, that could induce ovarian oocyte maturation and spawning in several seastar species, albeit some species-specificity was noted (Mita, 2013a,b; Mita et al., 2015a,b; Mita, 2016; Mita and Katayama, 2016). Also, a synthetic *Asterias rubens* and *Asterias amurensis* RGP has been produced and functionality determined through oocyte maturation (Mita et al., 2015a,b; Lin et al., 2017). No recombinant RGP had been described.

In this study, we explored the differential expression of RGP in COTS RNC and sensory tissues, then generated a biologically active recombinant COTS RGP using a yeast expression system. The recombinant COTS RGP is capable of inducing oocyte maturation and ovulation *in vitro*.

2. Materials and methods

2.1. COTS sample collection and RNA-seq

Adult COTS were collected from the Great Barrier Reef off the coastline of Cairns by the Australian Marine Park Tourism Operators (AMPTO) divers during the non-reproductive (June) and reproductive season (December). Biopsy of the gonad (described in detail further on) was used to determine sex and reproductive maturation, then RNC was taken from female COTS and stored in RNAlater solution (Life Technologies) at −80 °C until RNA isolation. Total RNA was extracted from tissues using Trizol (Invitrogen) following the manufacturer's instructions. RNA concentration and integrity were measured by Nanodrop spectrophotometry (Thermo Scientific) and then integrity was further assessed by agarose gel visualisation. Approximately 1 μg total RNA for each sample was sent to the Australian Genomic Research Facility (Brisbane) for library preparation and sequencing using the Illumina HiSeq 2500 platform to generate 100 base-pair single-end reads. Raw sequence data for female COTS RNC were deposited in NCBI under SRP186660. Raw sequence data for the female COTS tube feet and sensory tentacle was obtained from Roberts et al. (2017).

RNA-seq quantitative analysis was conducted using the CLC Genomics Workbench (v8.0; Qiagen) with mapping against the COTS genome and annotation files (http://marinegenomics.oist.jp) (Hall et al., 2017) using the standard in-built parameters for experimental groups. Sample comparisons (n = 3) were: i) female reproductive RNC *vs* female non-reproductive RNC, ii) female sensory tentacle *vs* female RNC, iii) female tube feet *vs* female RNC. An 'Exact Test', performed using the CLC Empirical analysis of DGE tool (Robinson and Smyth, 2008), was also performed with genes considered significantly differentially expressed (*P*-value of < 0.05).

2.2. Recombinant RGP plasmid construction and transformation

The COTS mature RGP A- and B-chain sequence (Hall et al., 2017; Smith et al., 2017), separated with a histidine linker encoding GSGS-HHHHHHGSGS, was inserted into the pPIC9K vector (Genscript Biotech Company). The recombinant RGP-pPIC9K was transformed into JM109 competent cells (Promega Corporation) and purified using a GeneJet plasmid Midiprep Kit (Thermo Scientific), then digested with the SalI restriction enzyme (Thermo Scientific). Standard electroporation was performed to transform the linear recombinant plasmid into competent yeast *Pichia pastoris* (strain SuperMan5, phenotype His^-, Biogrammatics) (Madden et al., 2015). Transformed cells were cultured by first growing on regeneration dextrose medium (RDB) agar plates for 4 days at 30 °C. Next, RDB plated colonies were inoculated into 96-well culture plates with 200 μl yeast extract; peptone; dextrose (YPD) solution, with 0 mg/ml, 1 mg/ml, and 2 mg/ml of Geneticin selective antibiotic (G418 disulfate, MERCK Company). Cultures were grown at 30 °C for 1–2 days before colony growth was assessed using a Multimode Plate Reader (EnSpire 2300, Perkin Elmer Singapore Ptd. Ltd., Singapore) at OD_{600}.

2.3. Induction of recombinant RGP protein expression

Target *P. pastoris* colonies (as determined by highest expression level in Geneticin G418) were inoculated and cultured in 200 ml of YPD solution, at 28 °C. Following 24 h, yeast was collected by centrifugation (3000 × *g*, 5 min) and resuspended in 400 ml of buffered minimal glycerol medium, then cultured for 24 h at 24 °C to achieve $OD_{600} > 1$. Following growth, cells were collected by centrifugation (3000 × *g*, 5 min) and resuspended in buffered minimal methanol medium and cultured for 3 days, to which 100% methanol was added to a final concentration of 0.5% daily. Cells were discarded by centrifugation (3000 × *g*, 10 min, 4 °C) and supernatant containing the secreted protein collected for analysis. As a negative control, *P. pastoris* yeast with no recombinant plasmid was subject to the same inoculation and culturing processes aforementioned and the supernatant collected.

2.4. Recombinant RGP His-tag purification and mass spectrometry

Supernatant containing the RGP was purified using Ni-NTA superflow agarose beads (QIArack kit, QIAGEN). Further purification of this eluent to remove imidazole was performed using an Amicon Ultra-15 centrifugal filter devices with a 3 KDa cut-off (MERCK) and protein concentration determined using a NanoDrop 2000 (Thermo Scientific). Using previously described methods (Ni et al., 2018), the purified recombinant RGP was digested with trypsin (Promega) and resuspended in 100 μl 0.5% formic acid (aq) (in MilliQ) water and analysed by LC-MS/MS on a ExionLC liquid chromatography system (AB SCIEX, Concord, Canada) coupled to a QTOF X500R mass spectrometer (AB SCIEX, Concord, Canada) equipped with an electrospray ion source. Twenty microliters of each sample were injected onto a 100 mm × 1.7 μm Aeris PEPTIDE XB-C18 100 uHPLC column (Phenomenex, Sydney, Australia) equipped with a SecurityGuard column for mass spectrometry analysis. Linear gradients of 5–35% solvent B over 10 min at 400 μl/min flow rate, followed by a steeper gradient from 35% to 80% solvent B in 2 min and 80% to 95% solvent B in 1 min were used for peptide elution. Solvent B was held at 95% for 1 min for washing the column and returned to 5% solvent B for equilibration prior to the next sample injection. Solvent A consisted of 0.1% formic acid (aq) and solvent B contained 100% acetonitrile/0.1% formic acid (aq). The ionspray voltage was set to 5500 V, declustering potential (DP) 100 V, curtain gas flow 30, ion source gas 1 40, ion source gas 2 (GS2) 50 and spray temperature at 450 °C. The mass spectrometer acquired mass spectral data in an Information Dependant Acquisition, IDA mode. Full scan TOFMS data was acquired over the mass range 350–1400 and for product ion ms/ms 50–1800. Ions observed in the TOF-MS scan exceeding a threshold of 100 cps and a charge state of +2 to +5 were set to trigger the acquisition of product ion. The data was acquired and processed using SCIEX OS software (AB SCIEX, Concord, Canada). Biological triplicates were used for the analysis.

The LC-MS/MS data were imported to the PEAKS studio (Bioinformatics Solutions Inc., Waterloo, ON, Canada, version 7.0) with the assistance of MS Data Converter (Beta 1.3, http://sciex.com/software-downloads-x2110). *De novo* sequencing of peptides, database search and characterising specific PTMs were used to analyse the raw data; false discovery rate (FDR) was set to ≤1%, and $[-10 * \log(p)]$ was calculated accordingly where p is the probability that an observed match is a random event. The PEAKS used the following parameters: (i) precursor ion mass tolerance, 0.1 Da; (ii) fragment ion mass tolerance, 0.1 Da (the error tolerance); (iii) tryptic enzyme specificity with two missed cleavages allowed; (iv) monoisotopic precursor mass and

fragment ion mass; (v) a fixed modification of cysteine carbamidomethylation; and (vi) variable modifications including lysine acetylation, deamidation on asparagine and glutamine, oxidation of methionine and conversion of glutamic acid and glutamine to pyroglutamate.

The conformation of the recombinant COTS RGP was built as a linear structure using the LEAP module of AMBER 14 (Case et al., 2014). Molecular dynamic (MD) simulation was fully unrestrained and carried out in the canonical ensemble using the SANDER module. The ff14SB force field (Duan et al., 2003) was employed. Energy minimisation with 2500 steps was first performed to remove unfavourable contacts. The AMBER structure was then heated to 325 K over 50 ps to avoid being kinetically trapped in local minima, then subjected to unrestrained MD simulations at 325 K for the purpose of peptide equilibration. The structural information was sampled every 1 ps (i.e., 10,000 structures were calculated for 10 ns MD simulation). This MD simulation was continued until the root mean square deviation of structures within a reasonable long-time range was stable at/less than 3 to 4 Å. Then a lowest energy structure was determined and considered as the representative of the conformations simulated over this period. Visualization of the systems was effected using VMD software (Humphrey et al., 1996). MD simulation against NMR-confirmed human insulin-like-growth factor −1 structure as a template (Cooke et al., 1991) was carried out using Swiss-Model workspace (https://swissmodel.expasy.org/) using in-built parameters (Guex et al., 2009; Bienert et al., 2017; Waterhouse et al., 2018).

2.5. In vitro oocyte germinal vesicle breakdown (GVBD) and ovulation bioassay

Adult COTS were collected from the Northern sector of the Great Barrier Reef off the coastline of Cairns, Queensland Australia, by control divers employed by the Australian Marine Parks Tourism Operators (AMPTO). COTS were transported to the National Marine Science Centre at Southern Cross University (Coffs Harbour, NSW), then housed in an isolated saltwater protein skimmed aquarium kept at 26 °C. Sex determination and gonadal (ovarian) maturation was measured by biopsy through a small incision on the COTS body wall meeting the proximal portion of the arm, then removal of a small fragment of gonad. Oocyte maturation stage I-IV was determined by microscopic examination measurements previously described (Takahashi and Kanatani, 1981), whereby mature stage oocytes were at > 200 µm diameter. Ovarian fragments containing stage V matured oocytes were isolated and washed of extruded oocytes using a small mesh sieve (size < 100 µm) and transferred into 96-well microplates containing 80 µl of test or control media. Extruded oocytes separated following the sieve procedure were transferred to a separate 96-well plate for treatment under the same conditions.

Recombinant COTS RGP was tested at 0.2, 0.02 and 0.002 µg/µL final concentration in filtered UV-treated seawater (FSW, ~34.5 ppt salinity, pH ~ 8.28). As negative controls, FSW was used, as well as supernatant collected from a yeast (*P. pastoris*) culture that did not contain the RGP construct. Radial nerve extract (RNE; final concentration of 0.20 µg/µL) and 10^{-5} M 1-MeAde in FSW were used as positive controls. RNE preparation followed methods previously described in sea cucumbers (Chieu et al., 2018). Six replicates were performed using two female COTS. Ovarian fragments were incubated in test media at ambient temperate (25 °C) for 1 h and observed at 5 min intervals using a light microscope (Leica DM550 microscope with Leica camera). Oocytes final maturation was determined by observation of GVBD and/or ovulation of eggs from ovarian fragment.

2.6. Fertilization and development of COTS larvae

Adult male COTS gonadal fragments were removed and through mechanical disruption the sperm cells were collected into a shallow petri dish containing a small volume of FSW. Approximately 5 µl of sperm solution was added to oocytes previously treated with recombinant RGP. Oocytes were monitored under a microscope (Leica stereomicroscope) for development/presence of a follicular envelope, which is an indicator of successful fertilization. Fertilized eggs were viewed at 3, 4 and 16 h post-fertilization (hpf) for continued development from a blastomere through to a blastula. The blastula was then transferred into drip filtration larval rearing pots (in FSW conditions as mentioned prior) and left until 7 days post-fertilization (dpf). These were viewed under a microscope to confirm development through to larval stage.

3. Results and discussion

3.1. Differential gene expression of RGP

In COTS, the RNC contains a large repertoire of neuropeptides and small molecule neurotransmitter molecules (Smith et al., 2017, 2018). The sensory tentacles are one of the few tissues outside of the RNC that contain apparent higher levels of some neuropeptides, including *RGP*. The sensory tentacles also contain numerous G protein-coupled receptors (GPCRs) thought to be chemosensory (Roberts et al., 2017), which likely activate an internal neuropeptide signalling system. To help validate *RGP* gene expression data in COTS tissues, we first performed quantitative RNA-seq of COTS RNC between reproductive and non-reproductive stages. We found a positive fold-change in *RGP* expression during the reproductive season, although not significant (Fig. 1A). A similar level of *RGP* expression throughout the seasons is consistent with what had been suggested in the literature with *A. pectinifera* (Mita et al., 2011a,b; Mita, 2013a,b; Mita et al., 2014; Ikeda et al., 2015). We next assessed *RGP* expression in RNC compared to the COTS sensory tissues, the tube feet and sensory tentacles (during their non-reproductive stage). We found a significant positive fold-change for expression in the sensory tentacles and a significant negative fold-change in the tube feet (Fig. 1B). This finding suggests that in seastars, RGP could be an important regulator of sensory processes.

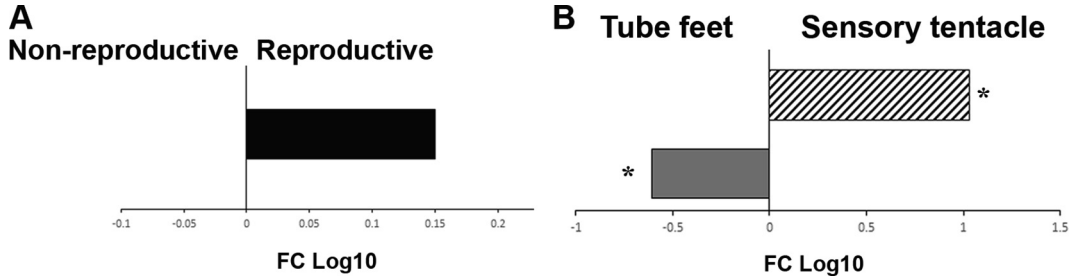

Fig. 1. RNA-seq differential expression of COTS *RGP*. (A) RNA-seq differential expression [fold change (FC log10)] of *RGP* in female radial nerve cord during reproductive compared to non-reproductive season. (B) RNA-seq differential expression [fold change (FC log10)] of *RGP* in female COTS radial nerve cord compared to sensory tissues during non-reproductive season. * indicates significant FC log10 of $p \leq 0.05$.

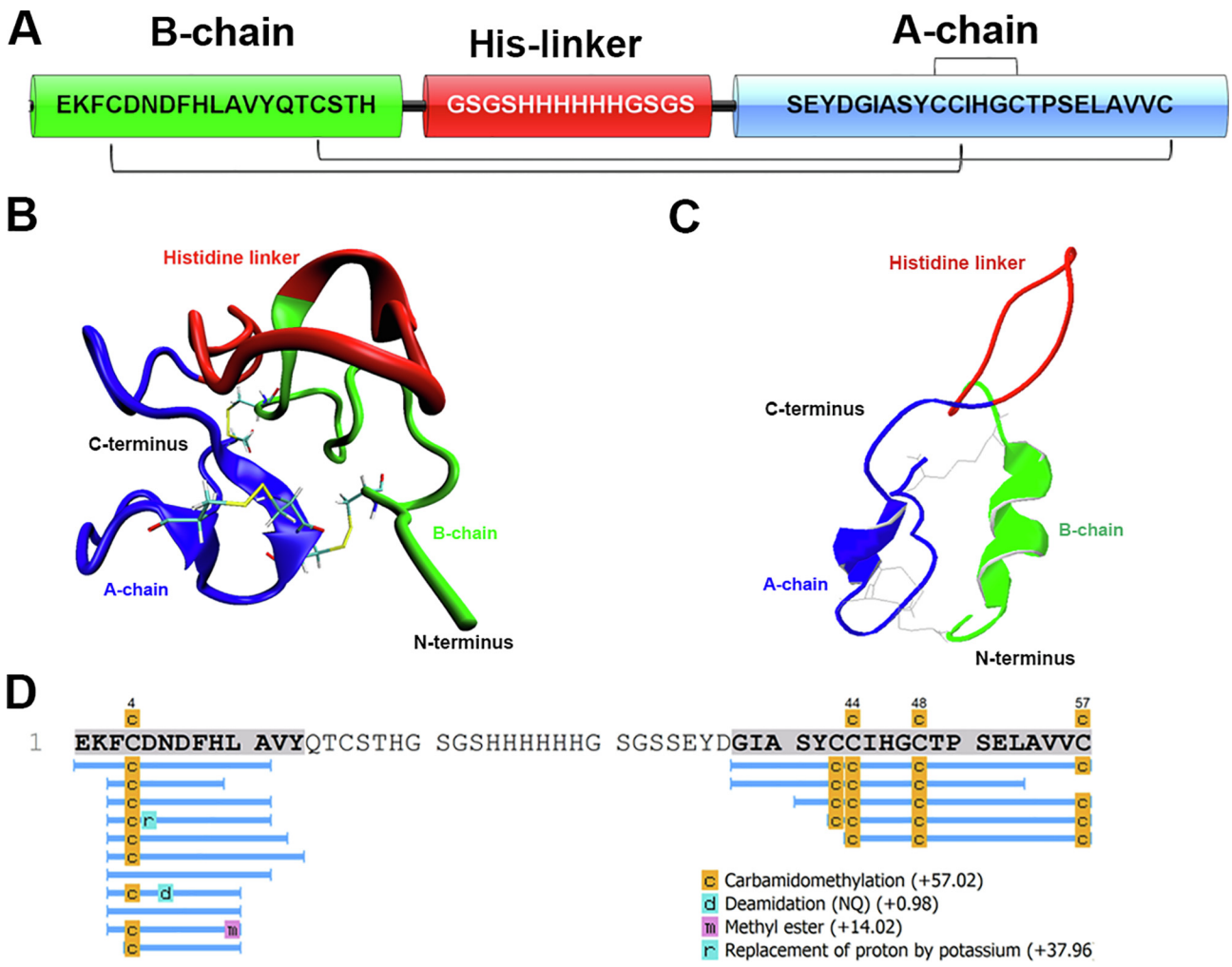

Fig. 2. Recombinant COTS RGP construct and mass spectrometry identification. (A) Schematic representation of the COTS RGP construct, showing B-chain and A-chain connected by a histidine (His) linker. Cysteine disulphide bridging indicated beneath chains. (B) Molecular Dynamic (MD) simulation model of recombinant COTS RGP. B-chain (green), A-chain (blue), histidine linker (red). Ribbon arrowheads indicate helices (β-sheet). (C) MD simulation of recombinant COTS RGP construct using NMR-confirmed structure of a human insulin-like-growth factor 1 [AAX36953.1] as a template. Ribbon arrowheads indicate helices (α-helix). (D) COTS RGP sequence demonstrating MS peptide coverage (blue underline).

3.2. Production of a recombinant COTS RGP

The production of a recombinant RGP is more cost efficient than production of synthetic RGP and, therefore, allows for relatively cheap production of quantities suitable for large-scale *in vivo* functional assays. Relaxin/insulin-like peptides have traditionally faced challenges during synthesis in heterologous systems due to the requirement for complex post-translational modifications (PTMs). The COTS *RPG* construct encodes a mature B-chain and A-chain, and with a histidine linker (Fig. 2A), this overcomes the requirement for precursor protein cleavage. A bacterial expression system, although cheaper, is generally less efficient in producing active recombinant heterodimeric proteins (Okuno et al., 2002). In addition, based on the previous development of recombinant insulin-like peptides that also contained internal linkers (Aizen et al., 2007, 2016), as well as a priority for correct disulphide bonding (Aizen et al., 2007; Chen et al., 2012; Sanchis-Benlloch et al., 2017), we chose the *P. pastoris* yeast system to produce recombinant COTS RGP. Following COTS *RGP* construct introduction into the yeast expression system, purification was facilitated through the histidine linker. This recombinant COTS RGP had a predicted molecular weight of 5.6 kDa.

The molecular dynamic (MD) simulation model using AMBER14 of recombinant COTS RGP (Fig. 2B) was supported by the relatively stable potential energy and backbone root mean square deviation. The histidine linker lies clearly outside the active region. Also, an MD simulation utilising the structure (based on nuclear magnetic resonance) of the human insulin-like-growth factor 1 (Cooke et al., 1991) as a template, confirms the active peptide is likely uninterrupted by the histidine linker (Fig. 2C). A minor difference between the two COTS RGP models occurs within the active peptide structure, indicating A-chain β-sheet or α-helices. This discrepancy could be later clarified through circular dichroism spectrometry, nuclear magnetic resonance or x-ray crystallography of the recombinant COTS RGP.

After expression and purification, mass spectrometry confirmed that the purified product was recombinant COTS RGP (Fig. 2D). With only a few *de novo* peptides identified, we predict that the final yield is of high purity. Recombinant COTS RGP yielded approximately 0.7 mg/l of culture, which is comparable to a recombinant yellowtail kingfish FSH produced using this system (i.e. ~0.4 to 0.9 mg/l) (Sanchis-Benlloch et al., 2017). However, there is scope for optimisation for increased yield based on the outcome of a previous study that generated 2 mg/L of a recombinant Japanese eel FSH (Kamei et al., 2003), or up to ~300 mg/L (90% purity) of a recombinant *Streptomyces* beta-lactamase inhibitory protein (Law et al., 2018) within a *P. pastoris* expression system. By increasing our yeast cell biomass or moving to an alternate yeast strain could potentially achieve increased yields. Nonetheless, our

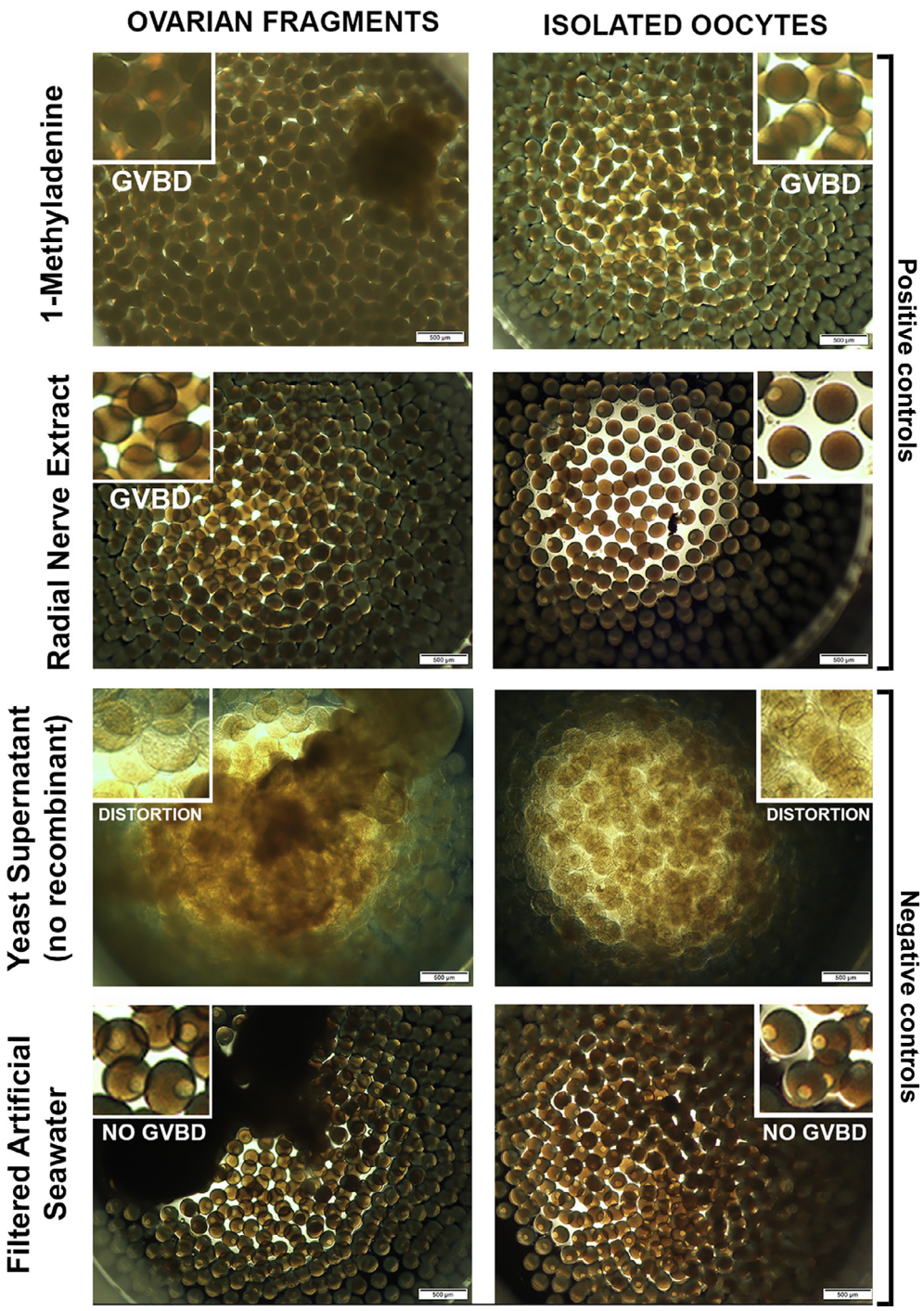

Fig. 3. Bioassay of ovarian fragments exposed to control stimulants at 1 h post-treatment. Positive controls: 1-Methyladenine (10^{-5} M) and radial nerve extract (0.2 µg/µl) with oocytes encapsulated in ovarian lobe and isolated from ovarian lobe. Negative controls: yeast supernatant extract with no recombinant peptide and filtered artificial seawater with oocytes encapsulated in ovarian lobe and isolated from ovarian lobe. GVBD, germinal vesicle breakdown.

current yield of recombinant COTS RGP was sufficient for *in vitro* experimental analysis.

3.3. In vitro GVBD bioassay with recombinant COTS RGP

Positive and negative controls were performed to assess COTS oocyte GVBD (Fig. 3). For positive controls, 1-MeAde and RNE were tested. The 1-MeAde resulted in complete GVBD (~100%) for oocytes that were still encapsulated within the ovarian fragments, as well as oocytes isolated from the ovarian fragments (also the common practice for *in vitro* fertilization and larval rearing of seastars and other echinoderms) (LÉOnet et al., 2009; Byrne et al., 2010; Haraguchi et al., 2016; Kamya et al., 2017). RNE at a final concentration of 0.2 µg/µL did also yield 100% GVBD in oocytes encapsulated within the ovarian fragment followed by ovulation, but only ~20% GVBD of oocytes isolated from ovarian follicle cells. The negative control using supernatant from yeast not containing the RGP construct resulted in complete distortion (distorted shape and border) of encapsulated oocytes, with rupturing of the ovarian follicle and the oocytes isolated from the ovarian fragment. The FSW negative control resulted in 0% GVBD of oocytes that were both encapsulated in ovarian fragment and oocyte isolated from ovarian fragment. Also, no ovulation occurred in both

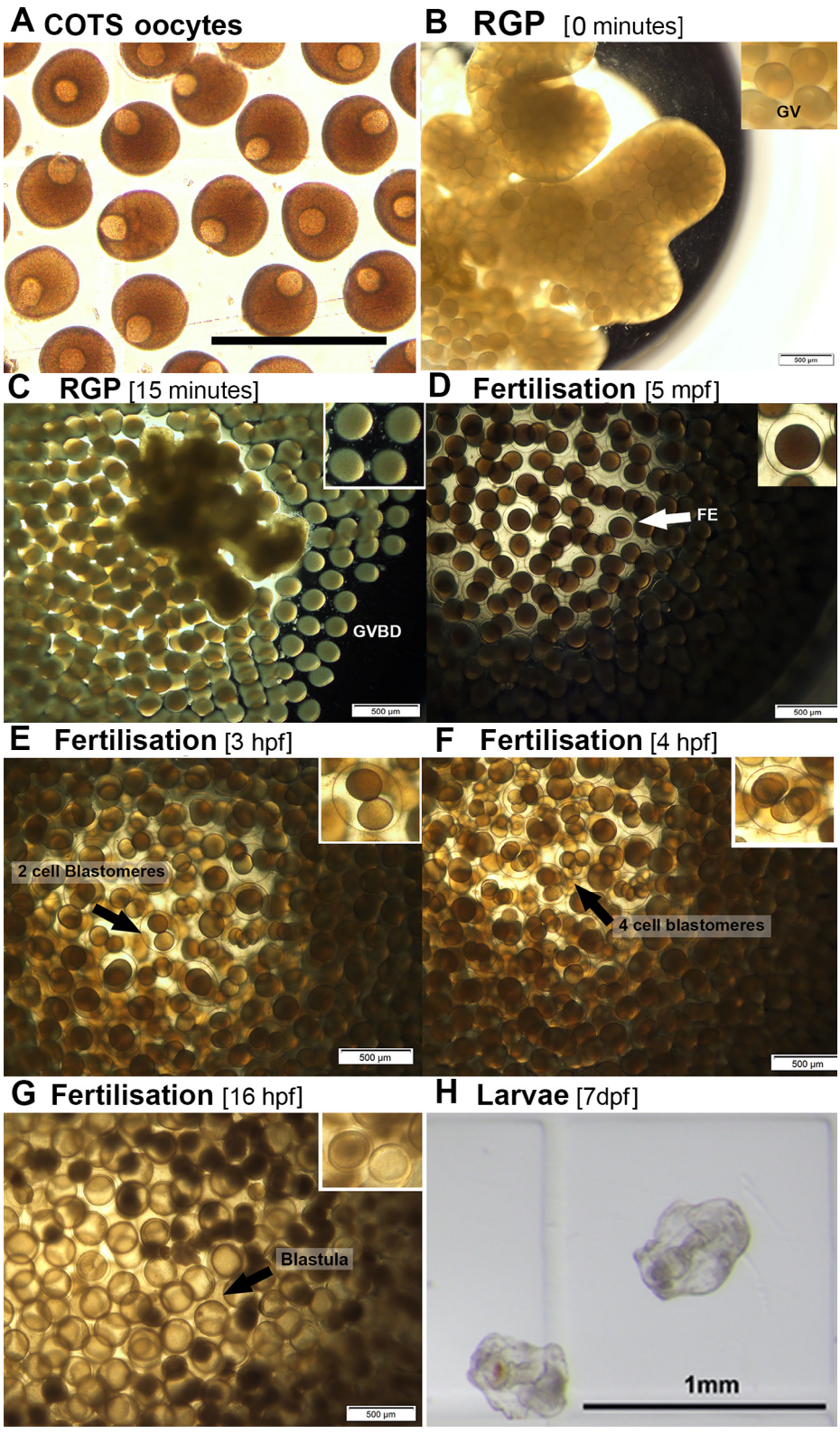

Fig. 4. Bioassay of ovarian fragments exposed to recombinant COTS RGP followed by fertilization and development. (A) Confirmation of oocyte development stage V as determined by oocyte diameter. Scale bar represents 500 µm. (B) Ovarian fragment with oocytes encapsulated at time-point 0 of RGP administration. Inset shows oocyte with visible germinal vesicle (GV). (C) Oocytes expelled from ovarian fragment following ovulation. GVBD, germinal vesicle breakdown (inset, magnified). (D) Fertilised oocytes with fertilization envelope (FE) present at 5 mpf (inset, magnified). (E) Development at 3 hpf showing 2-cell blastomeres apparent (inset, magnified). (F) Development at 4 hpf with 4-cell blastomeres apparent (inset, magnified). (G) Development at 16 hpf at blastula stage (inset, magnified). (H) Larval development at 7 dpf. Each larva measure approximately 0.5 mm in length.

negative controls.

Recombinant COTS RGP was tested for the induction of oocyte GVBD and ovulation using ovarian fragments isolated from female mature COTS containing mature oocytes (Fig. 4A). The oocytes encapsulated within the ovarian fragments all present germinal vesicles (GVs) at time-point 0 (Fig. 4B). Recombinant COTS RGP at final concentrations of 0.20, 0.02 and 0.002 µg/µL resulted in ~100% GVBD, and then ovulation from the ovarian fragment (Fig. 4C). GVBD was not observed in isolated oocytes, with the exception of approximately < 10 oocytes in treatment wells, which may be due to incomplete removal of ovarian follicle cells during preparation.

Ovarian fragments treated with recombinant COTS RGP underwent ovulation within 15 min post-treatment. This was evident by observation of oocyte expulsion until the ovarian lobes were completely spent

(Fig. 4C, Supplementary Video 1). Following ovulation, it seemed that 100% of eggs had undergone GVBD and upon application of sperm, these were noted to have fertilization envelopes in < 5 min, indicating successful fertilization (Fig. 4D). Following fertilization, observations were taken at 3 and 4 hpf and monitored for development. From then, 2-cell and 4-cell blastomeres were observed (Fig. 4E and F), with blastula apparent at 16 hpf (Fig. 4G). Embryos were transferred to larval rearing pots and observed at 7 dpf, showing development of larvae to approximately 0.5 mm in length (Fig. 4H). The maturation of oocytes within ovarian fragments with the recombinant RGP is consistent with the suggestion that the RGP receptor is expressed at the ovarian follicle cell membrane. Oocytes free of ovarian follicle cells did not undergo GVBD.

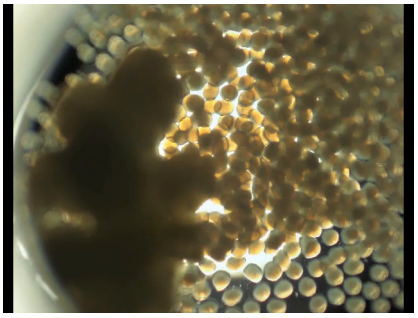

Supplementary Video 1.

3.4. Conclusions

Recombinant RGP was produced using a yeast expression system, with a high yield and predicted accurate post-translational folding which was capable of inducing oocyte maturation and ovulation *in vitro* at the tested concentrations of 0.2, 0.02, 0.002 µg/µL in female adult COTS that have mature gonads. Further testing *in vitro* using gonad at varying stages of maturation as well as *in vivo* studies using whole animals will further expand on our understanding of the RGP neuroendocrine system, receptor-ligand expression and interaction as well as exogenous chemical detection of RGP. This knowledge will advance applications for echinoderm aquaculture and contribute to the efforts to control future outbreaks of COTS.

Acknowledgments

The authors thank the GeneCology Research Centre for support with laboratory facilities. We also thank Josephine Nocillado and Peter Palma for their guidance in the laboratory with production of the recombinant RGP. Thanks to Tianfang Wang for performing the MS/MS analysis. We also thank the Dworjanyn laboratory team members at the National Marine Science Centre, Southern Cross University, Coffs Harbour NSW Australia, for access and assistance to COTS, larval rearing tanks and the use of equipment.

Funding

This work was supported financially by the GeneCology Research Centre and the Faculty of Science and Engineering at the University of the Sunshine Coast (USC), Queensland Australia. Funding was supported by an Australian Postgraduate Award scholarship to Meaghan K Smith.

Declaration of Competing Interest

None.

References

Aizen, J., et al., 2016. Production of recombinant insulin-like androgenic gland hormones from three decapod species: In vitro testicular phosphorylation and activation of a newly identified tyrosine kinase receptor from the Eastern spiny lobster, *Sagmariasus verreauxi*. Gen. Comp. Endocrinol. 229, 8–18.
Aizen, J., et al., 2007. Tilapia follicle-stimulating hormone (FSH): immunochemistry, stimulation by gonadotropin-releasing hormone, and effect of biologically active recombinant FSH on steroid secretion. Biol. Reprod. 76 (4), 692–700.
Bienert, S., et al., 2017. The SWISS-MODEL repository—new features and functionality. Nucl. Acids Res. 45 (D1), D313–D319.
Byrne, M., et al., 2010. Sea urchin fertilization in a warm, acidified and high pCO2 ocean across a range of sperm densities. Mar. Environ. Res. 69 (4), 234–239.
Case, D.A., Babin, V., Berryman, J.T., Betz, R.M., Cai, Q., Cerutti, D.S., Cheatham, T.E., Darden, T.A., Duke, R.E., Gohlke, H., Goetz, A.W., Gusarov, S., Homeyer, N., Janowski, P., Kaus, J., Kolossváry, I., Kovalenko, A., Lee, T.S., Legrand, S., Luchko, T., Luo, R., Madej, B., Merz, K.M., Paesani, F., Roe, D.R., Roitberg, A., Sagui, C., Salomon-Ferrer, R., Seabra, G., Simmerling, C.L., Smith, W., Swails, J., Walker, Wang, J., Wolf, R.M., Wu, X., Kollman, P.A., 2014. AMBER 14. University of California, San Francisco, CA.
Chaet, A.M.R., 1959. Physiologic activity of nerve extracts. Biol. Bull. 117, 407–408.
Chen, J., et al., 2012. Production of recombinant orange-spotted grouper (*Epinephelus coioides*) follicle-stimulating hormone (FSH) in single-chain form and dimer form by *Pichia pastoris* and their biological activities. Gen. Comp. Endocrinol. 178 (2), 237–249.
Chieu, H.D., et al., 2018. In vitro oocyte maturation by radial nerve extract and early development of the black sea cucumber (*Holothuria leucospilota*). Aquaculture 495, 247–254.
Coles, R.G., et al., 2015. The Great Barrier Reef World Heritage Area seagrasses: managing this iconic Australian ecosystem resource for the future. Estuar. Coast. Shelf Sci. 153, A1–A12.
Cooke, R.M., et al., 1991. Solution structure of human insulin-like growth factor 1: a nuclear magnetic resonance and restrained molecular dynamics study. Biochemistry 30 (22), 5484–5491.
Dana, T., et al., 1972. *Acanthaster* Aggregations: Interpreted as primarily responses to natural phenomena. Pac. Sci. 26, 355–372.
De'ath, G., et al., 2012. The 27–year decline of coral cover on the Great Barrier Reef and its causes. PNAS 109 (44), 17995–17999.
Duan, Y., et al., 2003. A point-charge force field for molecular mechanics simulations of proteins based on condensed-phase quantum mechanical calculations. J. Comput. Chem. 24 (16), 1999–2012.
GBRMPA, 2017. Crown-of thorns starfish control guidelines. Townsville.
Guex, N., et al., 2009. Automated comparative protein structure modeling with SWISS-MODEL and Swiss-PdbViewer: a historical perspective. Electrophoresis 30 (S1), S162–S173.
Hall, M.R., et al., 2017. The crown-of-thorns starfish genome as a guide for biocontrol of this coral reef pest. Nature 544, 231.
Haraguchi, S., et al., 2016. Nucleotide sequence and expression of relaxin-like gonad-stimulating peptide gene in starfish *Asterina pectinifera*. Gen. Comp. Endocrinol. 227, 115–119.
Hirai, S., Kanatani, H., 1971. Site of production of meiosis-inducing substance in ovary of starfish. Exp. Cell Res. 67 (1), 224–227.
Humphrey, W., et al., 1996. VMD: visual molecular dynamics. J. Mol. Graph 14 (1) 33-38, 27-38.
Hunt, J., 2013. Great Barrier Reef coral loss and crown-of-thorns starfish. Austr. Canegrower 18, 12–13.
Ikeda, N., et al., 2015. Relaxin-like gonad-stimulating peptide is highly conserved in starfish *Asterina pectinifera*. Invertebr. Reprod. Dev. 59 (4), 224–229.
Johnson, D.B., et al., 1990. Evaluation of a crown-of-thorns starfish (*Acanthaster planci)* control program at Grub Reef (central Great Barrier Reef). Coral Reefs 9 (3), 167–171.
Kamei, H., et al., 2003. Expression of a biologically active recombinant follicle stimulating hormone of Japanese Eel *Anguilla japonica* using methylotropic yeast, *Pichia pastoris*. Gen. Comp. Endocrinol. 134 (3), 244–254.
Kamya, P.Z., et al., 2017. Indirect effects of ocean acidification drive feeding and growth of juvenile crown-of-thorns starfish, *Acanthaster planci*. Proc. R. Soc. B: Biol. Sci. 284(1856).
Kenyon, G., 2014. The starfish eating the reef. Wildlife Australia 51 (3), 30–32.
Law, K.H., et al., 2018. Efficient production of secretory *Streptomyces clavuligerus* beta-lactamase inhibitory protein (BLIP) in *Pichia pastoris*. AMB Express 8 (1), 64.
LÉOnet, A., et al., 2009. A new method to induce oocyte maturation in holothuroids (Echinodermata). Invertebr. Reprod. Dev. 53 (1), 13–21.
Lin, M., et al., 2017. Cellular localization of relaxin-like gonad-stimulating peptide expression in *Asterias rubens*: new insights into neurohormonal control of spawning in starfish. J. Comp. Neurol. 525 (7), 1599–1617.
Madden, K., et al., 2015. "Electroporation of *Pichia pastoris*." Genetic Transformation Systems in Fungi Volume 1. Fungal Biol. 87–91.
Mita, M., 2013a. Relaxin-like gonad-stimulating substance in an echinoderm, the starfish: a novel relaxin system in reproduction of invertebrates. Gen. Comp. Endocrinol. 181, 241–245.
Mita, M., 2013b. Release of relaxin-like gonad-stimulating substance from starfish radial nerves by ionomycin. Zool. Sci. 30 (7), 602–606.
Mita, M., 2016. Starfish gonadotropic hormone: Relaxin-like gonad-stimulating peptides. Gen. Comp. Endocrinol. 230–231, 166–169.
Mita, M., et al., 2015a. A new relaxin-like gonad-stimulating peptide identified in the

starfish *Asterias amurensis*. Gen. Comp. Endocrinol. 222, 144–149.
Mita, M., et al., 2015b. A gonad-stimulating peptide of the crown-of-thorns starfish, *Acanthaster planci*. Invertebr. Rep. Dev. 59 (4), 212–217.
Mita, M., Katayama, H., 2016. A relaxin-like gonad-stimulating peptide from the starfish *Aphelasterias japonica*. Gen. Comp. Endocrinol. 229, 56–61.
Mita, M., Nagahama, Y., 1991. Involvement of G-proteins and adenylate cyclase in the action of gonad-stimulating substance on starfish ovarian follicle cells. Dev. Biol. 144 (2), 262–268.
Mita, M., et al., 2014. Effect of relaxin-like gonad-stimulating substance on gamete shedding and 1-methyladenine production in starfish ovaries. Sexual Reproduction in Animals and Plants. Springer Japan, Tokyo.
Mita, M., et al., 2011a. Interaction of relaxin-like gonad-stimulating substance with ovarian follicle cells of the starfish *Asterina pectinifera*. Zool. Sci. 28 (10), 764–769.
Mita, M., et al., 2011b. Hormonal action of relaxin-like gonad-stimulating substance (GSS) on starfish ovaries in growing and fully grown states. Gen. Comp. Endocrinol. 172 (1), 85–89.
Morello, E.B., et al., 2014. Model to manage and reduce crown-of-thorns starfish outbreaks. Mar. Ecol. Prog. Ser. 512, 167–183.
Ni, G., et al., 2018. Comparative proteomic study of the antiproliferative activity of frog host-defence peptide caerin 1.9 and its additive effect with caerin 1.1 on TC-1 cells transformed with HPV16 E6 and E7. Biomed. Res. Int. 2018, 7382351.
Okuno, A., et al., 2002. Preparation of an active recombinant peptide of crustacean androgenic gland hormone. Peptides 23 (3), 567–572.
Roberts, R.E., et al., 2017. Identification of putative olfactory G-protein coupled receptors in Crown-of-Thorns starfish, *Acanthaster planci*. BMC Genomics 18 (1), 400.
Robinson, M.D., Smyth, G.K., 2008. Small-sample estimation of negative binomial dispersion, with applications to SAGE data. Biostatistics 9 (2), 321–332.
Sanchis-Benlloch, P.J., et al., 2017. In-vitro and in-vivo biological activity of recombinant yellowtail kingfish *(Seriola lalandi)* follicle stimulating hormone. Gen. Comp. Endocrinol. 241, 41–49.
Semmens, D.C., Elphick, M.R., 2017. The evolution of neuropeptide signalling: insights from echinoderms. Brief. Funct. Genomics 16 (5), 288–298.
Semmens, D.C., et al., 2016. Transcriptomic identification of starfish neuropeptide precursors yields new insights into neuropeptide evolution. Open Biol. 6 (2).
Smith, M., et al., 2018. Differences in small molecule neurotransmitter profiles from the Crown-of-Thorns Seastar radial nerve revealed between sexes and following food-deprivation. Front. Endocrinol.
Smith, M.K., et al., 2017. The neuropeptidome of the Crown-of-Thorns Starfish, *Acanthaster planci*. J. Proteomics 165, 61–68.
Taghert, Paul H., Nitabach, Michael N., 2012. Peptide neuromodulation in invertebrate model systems. Neuron 76 (1), 82–97.
Takahashi, K., Kanatani, H., 1981. Effect of 17β-estradiol on growth of oocytes in cultures ovarian fragments of the starfish, *Asterina pectinifera*. Dev. Growth Differ. 23 (6), 565–569.
Thalluri, K., et al., 2018. Synthesis of disulfide-rich heterodimeric peptides through an auxiliary N, N-crosslink. Commun. Chem. 1 (1), 36.
Tian, S., et al., 2016. Urbilaterian origin of paralogous GnRH and corazonin neuropeptide signalling pathways. Sci. Rep. 6, 28788.
Waterhouse, A., et al., 2018. SWISS-MODEL: homology modelling of protein structures and complexes. Nucl. Acids Res. 46 (W1), 296–303.